Ye et al. *glucagon* is essential for alpha cell transdifferentiation and beta cell neogenesis.

Supplementary Materials

Supplementary Figures

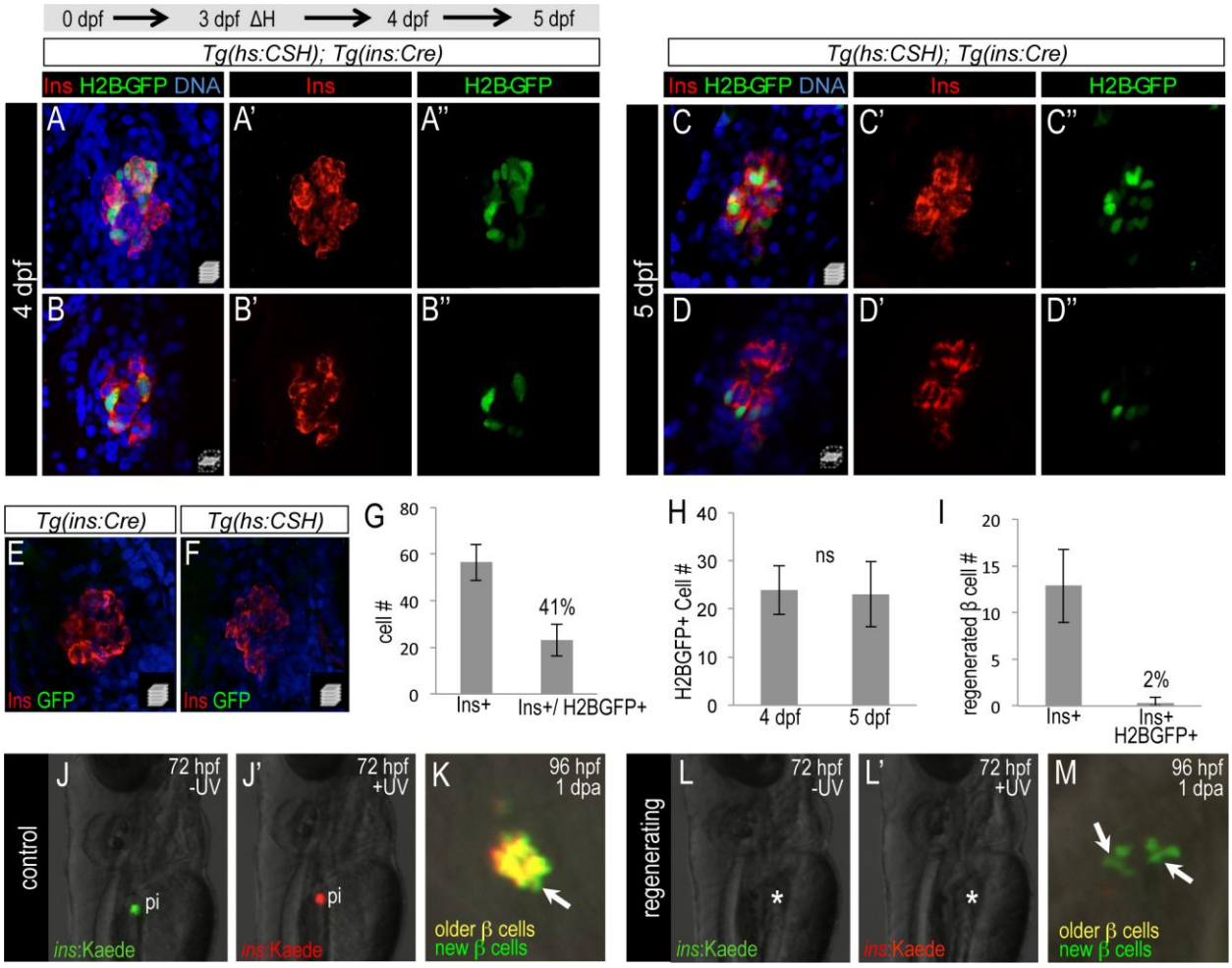

Figure S1. Pre-existing β cells do not contribute to β cell regeneration. (A-D) Confocal projections (A,C) and confocal planes (B,D) of *Tg(hs:CSH)*; *Tg(ins:cre)* islets at 4 dpf (A,B) and 5 dpf (C,D) that were heat shocked at 3 dpf and stained for insulin (red), GFP (green), and DNA (blue). Insulin^{+} cells were specifically labeled by H2B-GFP. (E, F) Confocal projections of 4 dpf *Tg(ins:cre)* (E) and *Tg(hs:CSH)* (F) islets showed no aberrant or leaky H2B-GFP fluorescence after heatshock. (G) Quantification of insulin^{+} and insulin^{+}/H2B-GFP^{+} cells at 4 dpf showed 41% of βcells were marked (*n*=11). (H) The number of labeled β cells remained constant from 4 to 5 dpf (*n*=7). (I) Quantification of total and H2B-GFP^{+} β cells in *the* regenerating islets represented in Fig 1I. Only ~2% of new βcells were labeled (*n*=13). (J-M) Epifluorescent images of *ins:Kaede; ins:CFP* larvae. (J) Green Kaede and (J')

converted red Kaede in the βcells of a 72 hpf larva. (K) A 96 hpf larva 24 hours after photo-conversion exhibited βcells present during UV exposure (yellow) as well as new βcells formed after the exposure (green only, arrow). (L) Neither green Kaede (L) nor converted red Kaede (L') are evident at 72 hpf after MTZ-ablation of βcells. (M) A 96 hpf photo-converted larvae 24 hours after photoconversion and cessation of MTZ treatment shows only new βcells (green, arrows).Student's t-test was used in H for statistical analysis.

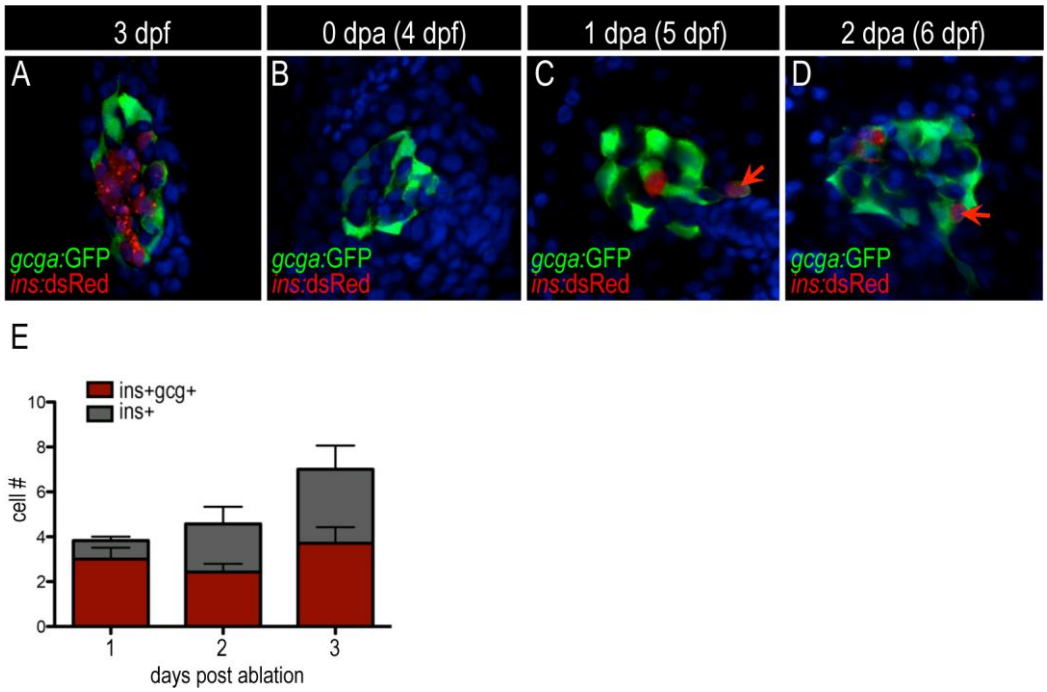

Figure S2. Emergence of *gcga:*GFP$^+$ *ins:*dsRed$^+$ dual hormone cells during regeneration. (A-D) Confocal planes of *Tg(gcga:GFP); Tg(ins:dsRed); Tg(ins:Flag-NTR)* islets in non-ablated 3 dpf (A), ablated 4 dpf (B), 1 dpa (C), and 2 dpa (D) larvae stained for DNA (blue). *gcga:*GFP$^+$ *ins:*dsRed$^+$ dual hormone expressing cells are marked by red arrows. (E) Quantification of *ins:*dsRed$^+$ single positive and *ins:*dsRed$^+$ *gcga:*GFP$^+$ dual positive cells in regenerating islets from 1 to 3 dpa (n≥3).

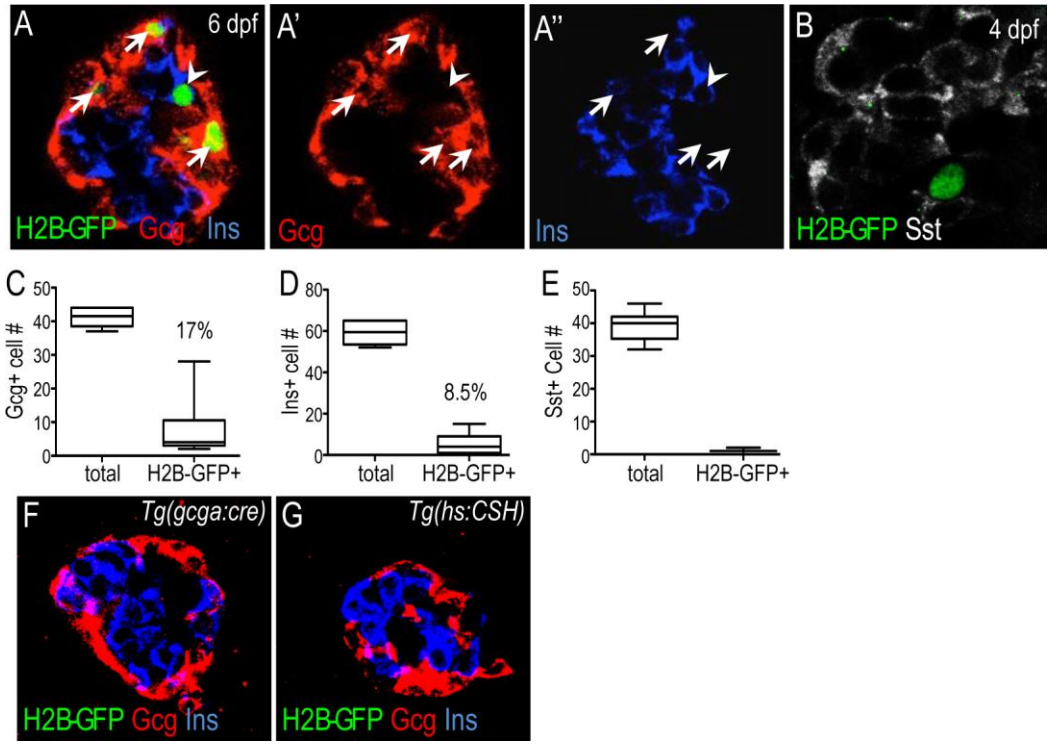

Figure S3. Characterization of *glucagon* promoter activity in *Tg(gcga:Cre)*. (A) Merged and single channel confocal planes of 6 dpf *Tg(gcga:cre);Tg(hs:CSH)* islets heat shocked at 3 dpf and stained for GFP (green), Insulin (blue) and glucagon (red). (B) Confocal plane of 4 dpf *Tg(gcga:cre);Tg(hs:CSH)* islet heat shocked at 3 dpf and stained for Somatostatin (white) and GFP (green). (C) Quantification of total glucagon^{+} and H2B-GFP^{+} glucagon^{+} cells in A shows that ~17% of αcells were marked (*n*=10). (D) Quantification of total Ins^{+} and H2B-GFP^{+} Ins^{+} cells in A shows that ~8.5% of βcells were marked (*n*=6). (E) Quantification of Sst+ and Sst+ H2B-GFP^{+} cells in B (*n*=11). (F-G) Confocal planes of 4 dpf *Tg(gcga:cre)* (F) and *Tg(hs:CSH)* (G) islets showed no aberrant or leaky H2B-GFP expression after heat shock.

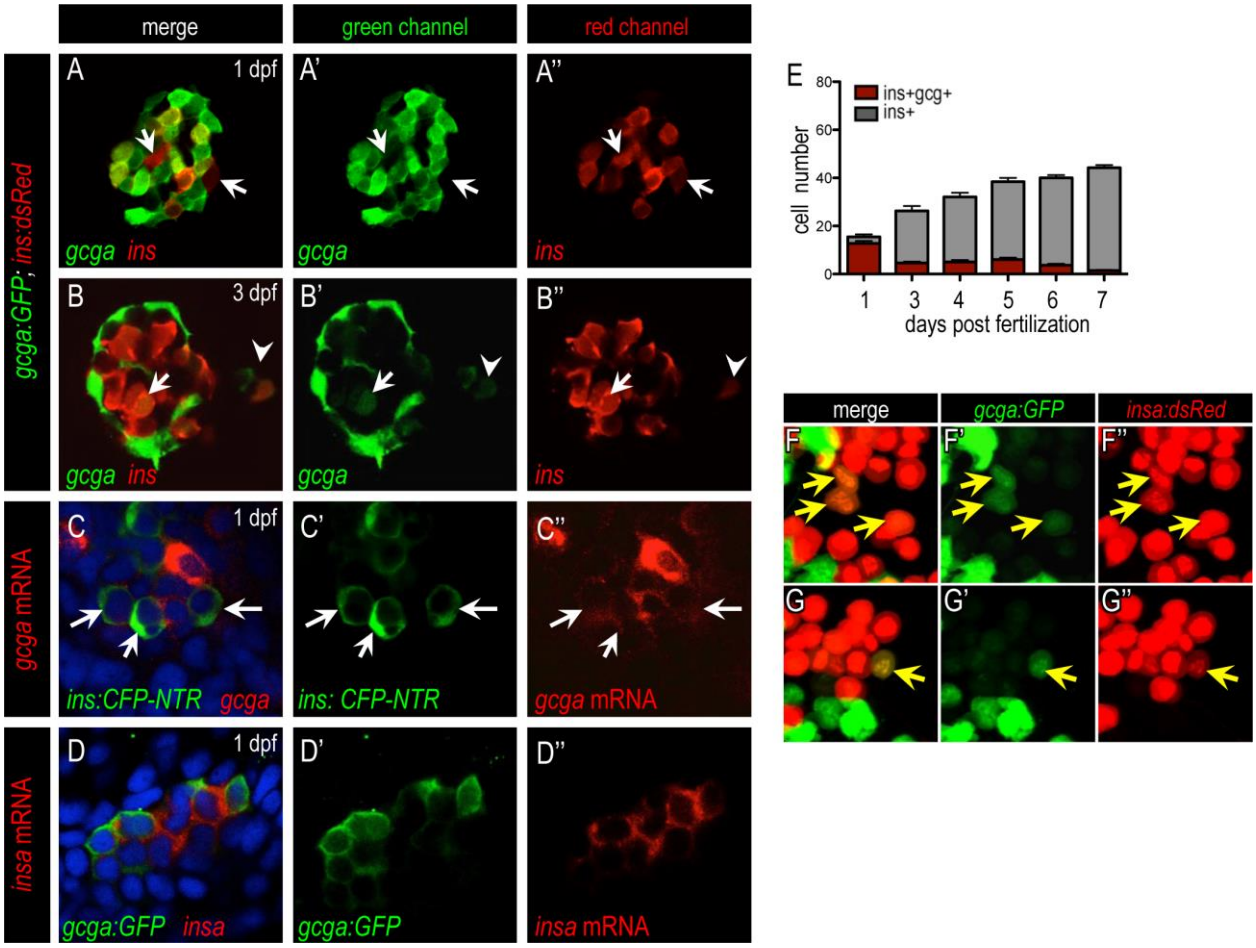

Figure S4. *ins+ gcga+* cells during early islet development. (A) Confocal planes of 1 dpf *Tg(gcga:GFP); Tg(ins:dsRed)* islet showed that the majority of *ins+* cells at 1 dpf are also *gcga+*. Single positive *insulin* expressing cells are indicated by arrows. (B) Confocal planes of 3 dpf *Tg(gcga:GFP); Tg(ins:dsRed)* islet showed *ins+ gcga+* cells in the principal islet (arrow) and *ins+ gcga+* newly formed βcells (arrowhead) in the extrapancreatic duct. (C-D) Merged and single channel confocal planes of fluorescent in situ hybridization (C) *proglucagon* (red) expressed in *ins+* cells (green) at 1 dpf in *Tg(ins:CFP-NTR)* islets immunostained for GFP (green). (D) *insulin* (red) expressed in *gcga+* cell(green) in 1 dpf *Tg(gcga:GFP)* islet immunostained for GFP (green). (E) Quantification of *ins+ gcga+* and *ins+* cells at 1 dpf through 7 dpf. *Tg(gcga:GFP); Tg(ins:dsRed)* islets showed a decrease of dual hormone-expressing cells with islet maturation.

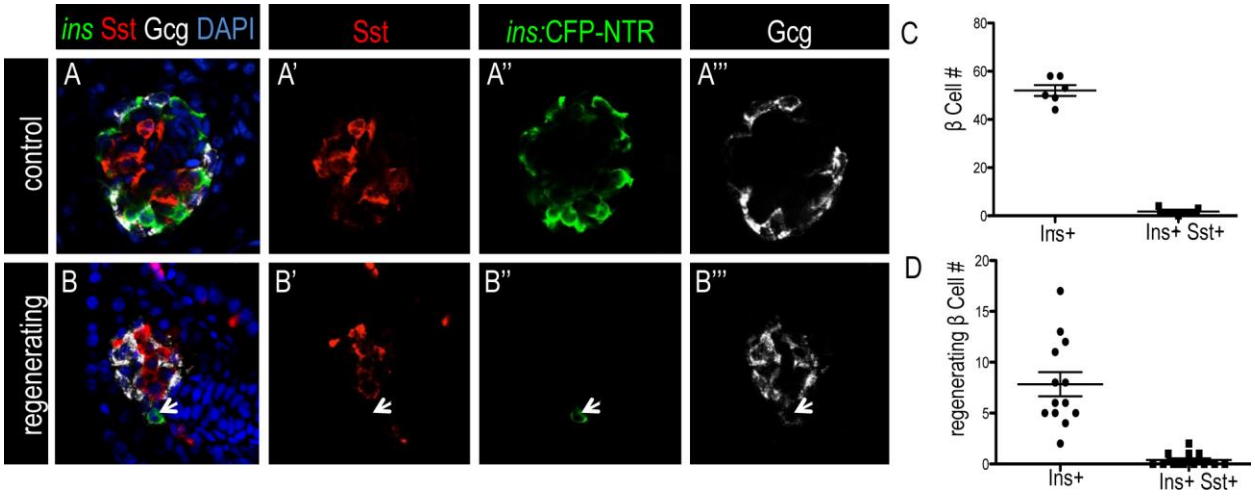

Figure S5. Insulin and somatostatin are rarely co-expressed in non-ablated or regenerating islets. (A-B’’’) Merged and single channel confocal images of 4 dpf *Tg(ins:CFP-NTR)* islets stained for CFP (green), somatostatin (red), and glucagon (white), that were not ablated (A), or ablated from 2-3 dpf (B). Regenerating *insulin*+ βcells (arrow) were rarely labeled. (C,D) Quantification of βcells and regenerated βcells that were *insulin*$^{+}$ or *insulin*$^{+}$ somatostatin^{+}.

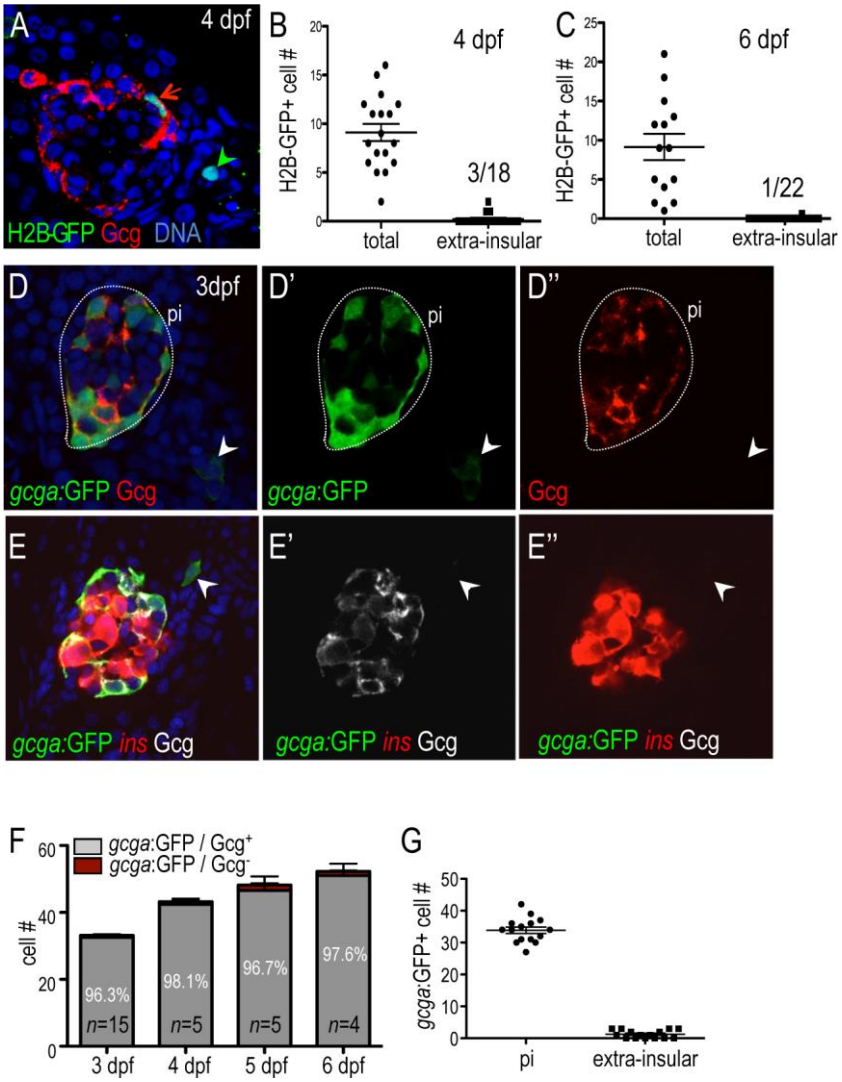

Figure S6. Characterization of *glucagon* promoter activity in extra-insular endocrine cells.

(A) Confocal Plane of 4 dpf *Tg(gcga:cre); Tg(hs:CSH)* islet heat shock at 3 dpf stained for Glucagon (red) and GFP (green). Green arrow head indicates Glucagon-H2B-GFP$^+$ Cells outside the islet. (B,C) Quantification of total and extra-insular H2B-GFP$^+$ cells in *Tg(gcga:cre);Tg(hs:CSH)* larvae heat shocked at 3 dpf. At 4 dpf (B), 3 out of 18 samples were found to have extra-insular H2B-GFP$^+$ cells. At 6 dpf (C), 1 out of 22 samples was found to have extra-insular H2B-GFP$^+$ cells. (D) Merged and single channel confocal planes of 3 dpf *Tg(gcga:GFP)* islets stained for GFP (green) and glucagon (red). Arrowhead indicates *gcga:GFP*$^+$ glucagon- cells in pancreatic duct region outside of principal islet. (E) Merged and single channel confocal planes of 3 dpf *Tg(gcga:GFP);Tg(ins:dsRed)* islets stained for GFP (green) ,dsRed (red) and Glucagon (white). Arrowhead indicates *gcga:GFP*$^+$ *ins*:dsRed$^-$Glucagon$^-$ cells in pancreatic duct region outside of principal islet. (F)

Quantification of *gcga:GFP*$^{+}$ glucagon^{-} and *gcga:GFP*$^{+}$ glucagon^{+} cell number in principal islet from 3 dpf through 6 dpf. The percent of *gcga:GFP*$^{+}$ glucagon^{-} cells is consistent but small. (G) Quantification of insular and extra-insular *gcga:GFP*+ cell numbers.

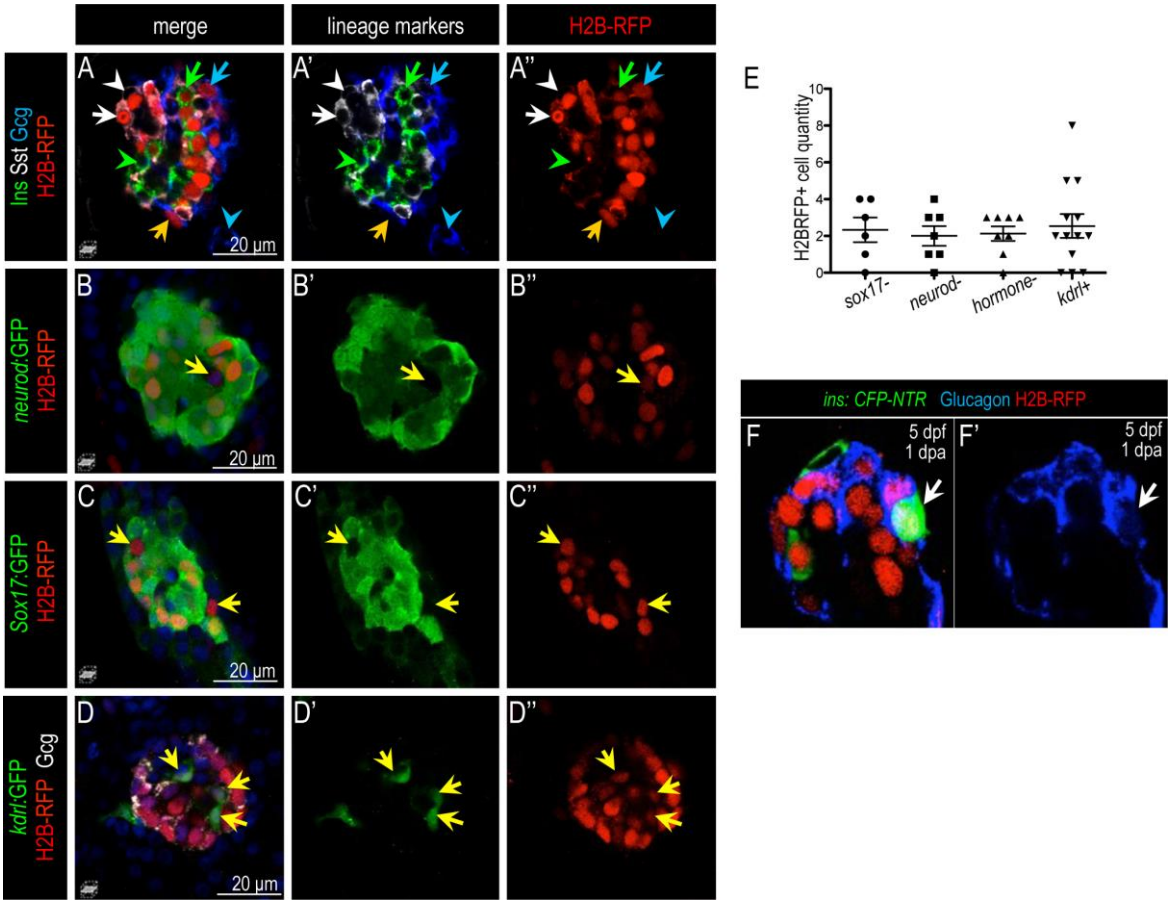

Figure S7. *H2B-RFP* label retaining assay marks early differentiated endocrine cells. (A-D) Confocal planes of islets labeled with H2B-RFP. (A) Wild type islet stained for Insulin (green), Somatostatin (white) and Glucagon (blue) at 5 dpf. There are 2 endocrine populations in the islet: H2B-RFP^{+} (arrows) and H2B-RFP^{-} (arrowheads). Yellow arrow indicates H2B-RFP^{+} cells in the islet lacking hormone staining. (B) *TgBAC(neurod1:*EGFP*)* islet stained for GFP (green) at 3 dpf. Yellow arrow indicates *neurod1*$^{-}$ H2B-RFP^{+} non-endocrine cells in the principal islet. (C) *Tg(sox17*:GFP*)* islet stained for GFP (green) at 3 dpf. Yellow arrows indicate *sox17*$^{-}$ H2B-RFP^{+} non-endodermal cells in the principal islet. (D) *Tg(kdrl:*GFP*)* islet region stained for GFP (green) and Glucagon (white) at 4 dpf. Yellow arrows indicate *kdrl:GFP*$^{+}$ H2B-RFP^{+} blood vessel cells in the principal islet. (E) Quantification of *sox17*$^{-}$ H2B-RFP^{+}, *neurod1*$^{-}$ H2B-RFP^{+}, and islet hormone (Ins/Gcg/Sst)$^{-}$ H2B-RFP^{+} cell quantities in the islet. (F) 1 dpa regenerating *Tg(ins:CFP-NTR)* islet stained for CFP (green) and glucagon (blue). The white arrow indicates a triply positive *ins*:CFP-NTR^{+} glucagon^{+} H2B-RFP^{+} βcell.

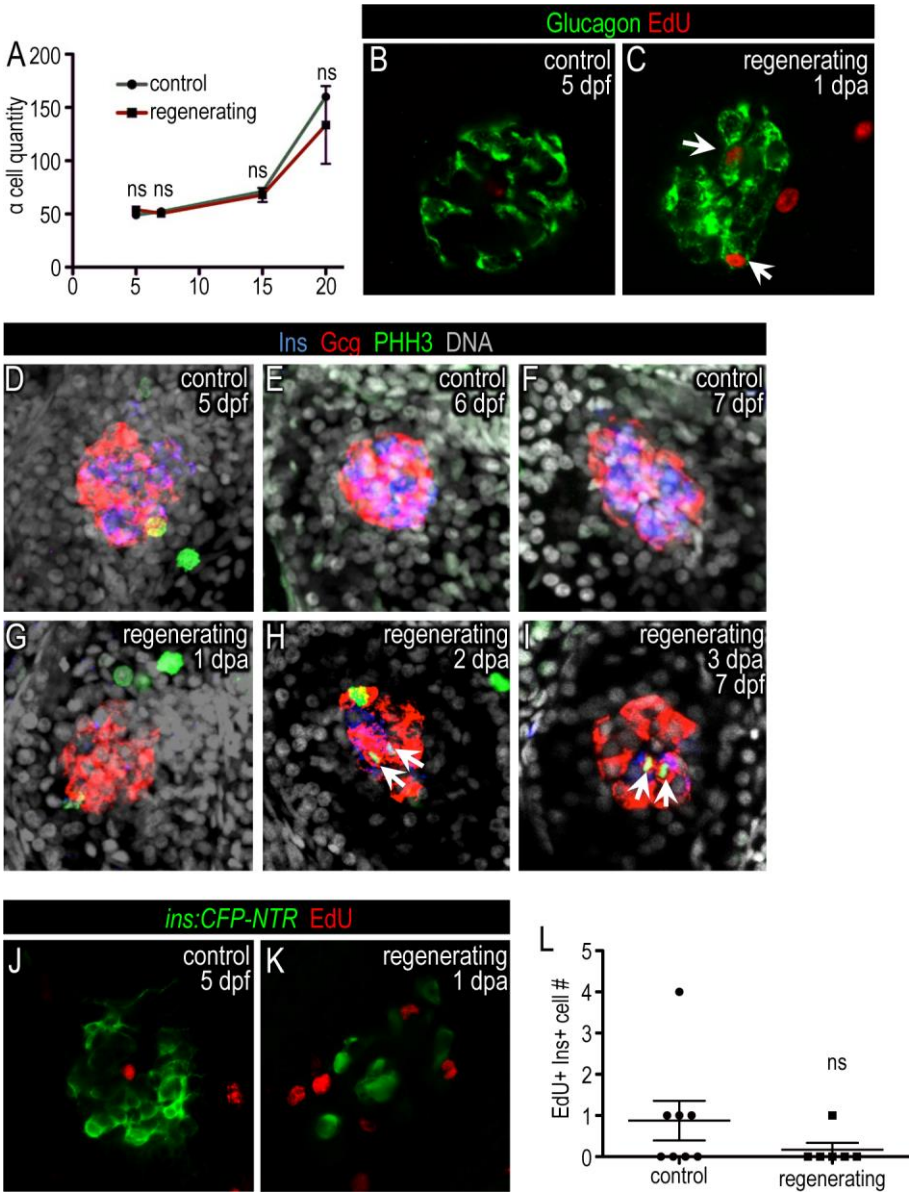

Figure S8. Proliferation of α cells but not β cells during β cell regeneration. (A) Quantification of αcell number between 5 dpf and 20 dpf in control (gray) and regenerating (red) islets ($n \geqq 3$). (B-C) Confocal planes of non-ablated (B) or 1 dpa (C) 5 dpf *Tg(ins:FlagNTR)* islets labeled with EdU (red) and stained for Glucagon (green). White arrows indicate Glucagon$^+$ EdU$^+$ cells in 1 dpa islet. (D-I) Confocal projections of *Tg(ins:CFP-NTR)* islets stained for phospho-histone H3 (green), glucagon (red), insulin (blue) and DNA (white) that were not ablated (D-F) or ablated from 3-4 dpf and regenerating (G-I). Islets were analyzed at 5 dpf (D,G), 6 dpf (E,H), and 7 dpf (F,I). No phospho-histone staining was observed in any non-ablated islet (n=21) and 17.6% of regenerating islets showed staining (n=17). (J-K) Confocal planes of non-ablated (J) or 1 dpa (K) 5 dpf

Tg(ins:CFP-NTR) islets labeled with EdU (red) and stained for GFP (green). (L) Quantification of $ins^{+}EdU^{+}$ cells in intact and ablated 5 dpf islets. Two-way ANOVA was used in A and Student's t-test was used in L for statistical analysis.

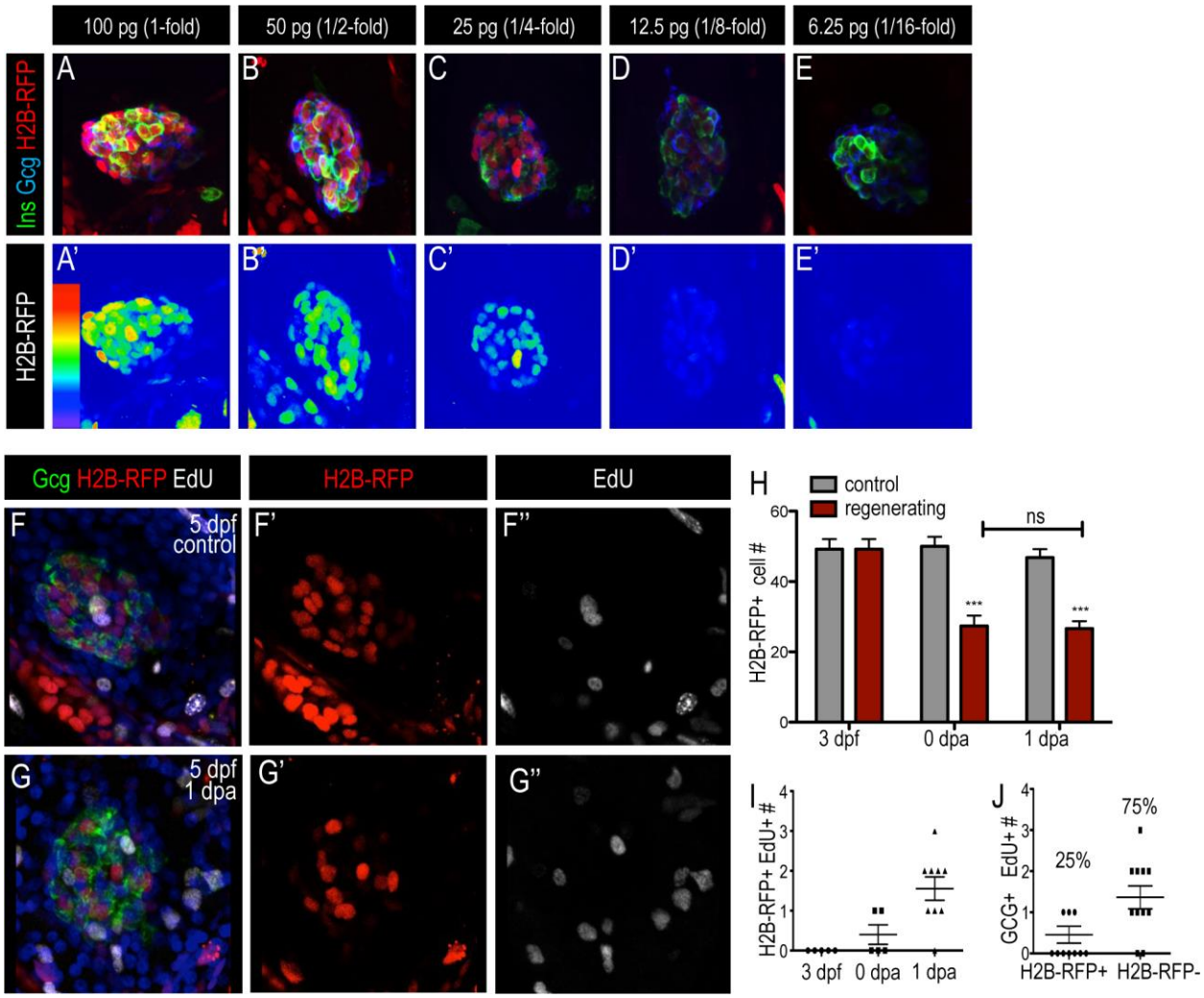

Figure S9. Proliferation of H2B-RFP$^+$ cells during regeneration does not dilute H2B-RFP mRNA. (A-E) Confocal projections of 5 dpf islets injected with decreasing amounts of *H2B-RFP* (red) mRNA that were immunostained for insulin (green) and glucagon (blue) to show endocrine differentiation. (A'-E') heat map representation of H2B-RFP fluorescence from confocal projections in A-E. Note that there is detectable H2B-RFP signal when mRNA was injected at the dose of 12.5 pg/embryo, which is an eightfold dilution. (F-G) Confocal projections of *H2B-RFP* mRNA injected 5 dpf control (F) and 1 dpa regenerating (G) islets that were labeled with EdU (white) for 1 hour, and stained for glucagon (green), RFP (red), and DNA (blue). (H) Quantification of total H2B-RFP$^+$ cells in islets from 3 dpf to 5 dpf in both intact islet (grey) and ablated islets (red). There is a significant decrease of total H2B-RFP$^+$ cell quantity in the islet during βcell ablation, but no difference of total H2B-RFP$^+$ cell number in the islet during regeneration between 0 dpa and 1 dpa. (I) Quantification of H2B-RFP$^+$ Edu$^+$ cell number during regeneration showed there are at most 2 Edu$^+$ H2B-

RFP^+ cells per islet during regeneration. (J) Quantification of H2B-RFP^+ and H2B-RFP^- Glucagon+ Edu^+ cell number in 1 dpa regenerating islets showed that 75% of proliferating α cells were H2B-RFP^-. Two-way ANOVA was used in H for statistical analysis.

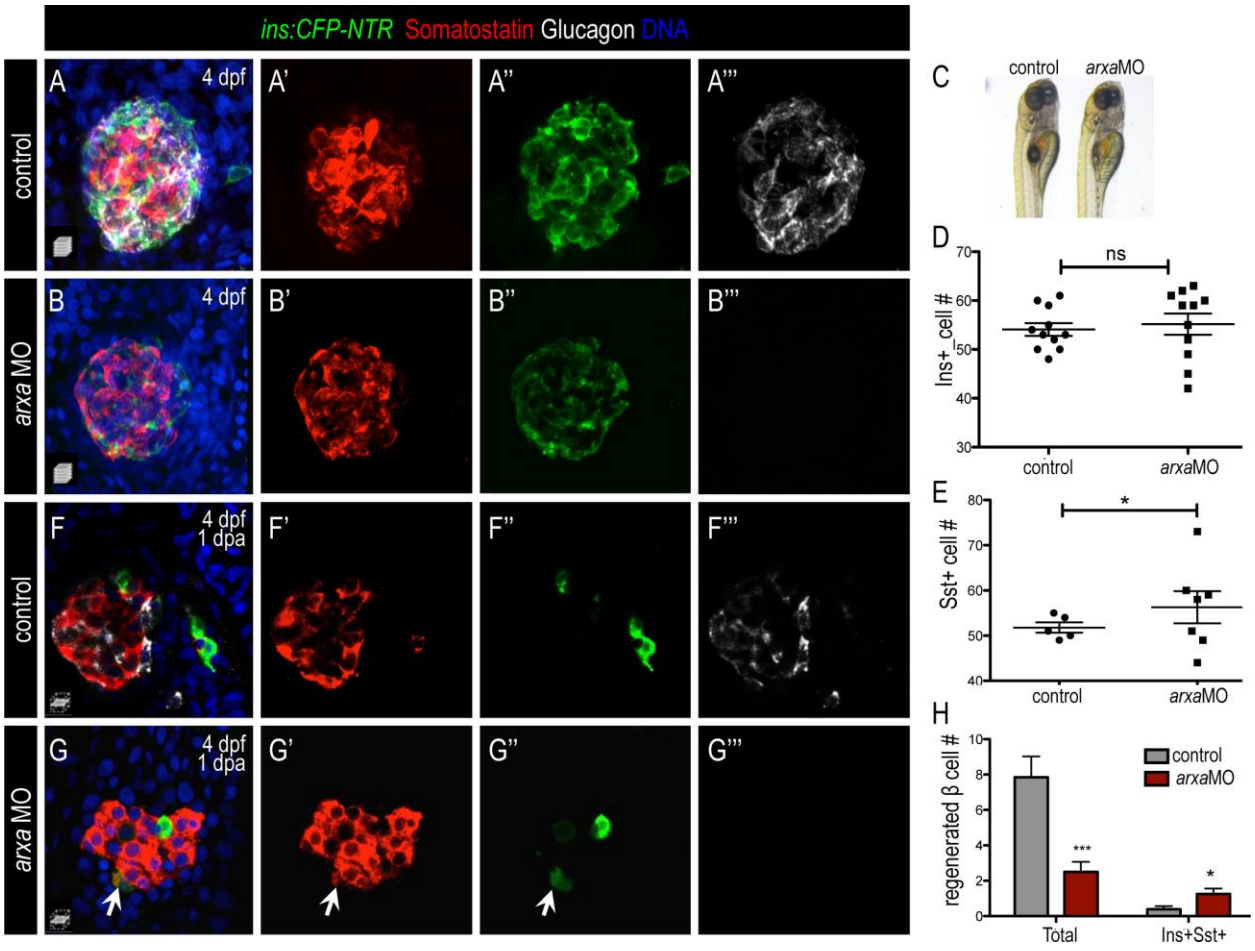

Figure S10. *arxa* knockdown induces the appearance of insulin/somatostatin co-expressing cells. (A-B) Confocal projections of 4 dpf control MO (A) and *arxa*MO- (B) injected *Tg(ins:CFP-NTR)* islets stained for somatostatin (red), glucagon (white) and GFP (green). (C) Control MO and *arxa*MO-injected 4 dpf larvae show no general developmental defects. (D-E) Quantification of total insulin$^+$ and somatostatin$^+$ cell number in 4 dpf control and *arxa*MO-injected larvae. (F-G) Confocal planes of 1 dpa control (F) and *arxa*MO-injected (G) *Tg(ins:CFP-NTR)* regenerating islets stained for somatostatin (red), glucagon (white) and GFP (green). White arrow in G indicates somatostatin$^+$ *insulin*$^+$ regenerating β cells in *arxa*MO-injected regenerating islet. (H) Quantification of total *insulin*$^+$ βcells and *insulin*$^+$ somatostatin$^+$ βcells in 1 dpa control and *arxa*MO-injected regenerating islets. Student's t-test was used in D,E, and H for statistical analysis.

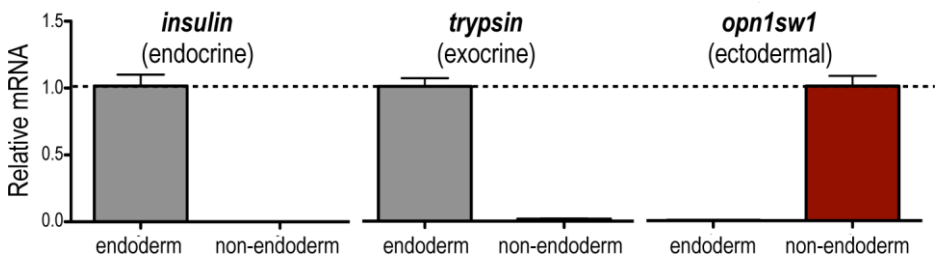

Figure S11. Endodermal organ cDNA preparations are enriched for endoderm. Quantitative PCR analysis on cDNA isolated from pools of dissected endodermal organs (pancreas, liver, intestine) and non-endodermal organs (the remainder of the larva). Preparations were tested for markers of the endocrine pancreas (*insa*), the exocrine pancreas (*trypsin*), and a non-endodermal opsin (*opn1sw1*). Virtually all of the *insa* and *trypsin* signal was limited to the endodermal fraction, while *opn1sw* was restricted to the non-endodermal fraction. *insa* and *trypsin* were normalized to the expression level in endoderm, while *opn1sw1* was normalized to non-endoderm. *n*=6 for all samples.

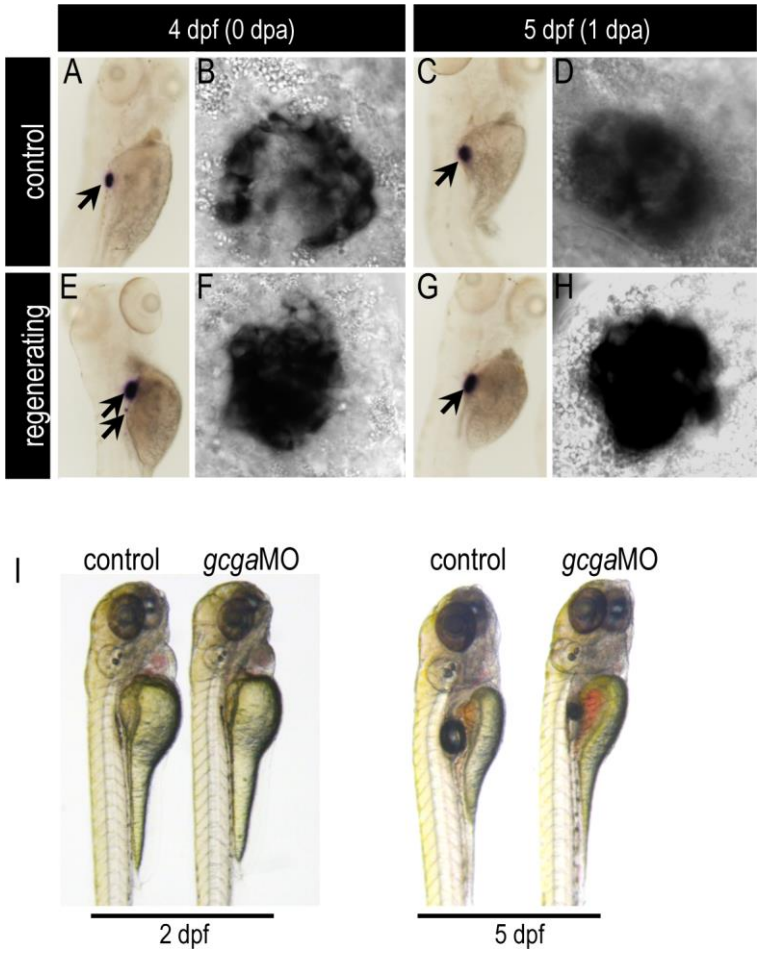

Figure S12. *glucagon* expression is increased in regenerating pancreata, but not is required for general embryonic development. Expression of *glucagon* revealed by *in situ* hybridization in non-ablated control (A-D), 0 dpa βcell-ablated (E,F), and 1 dpa regenerating (G,H) *Tg(ins:CFP-NTR)* islets at 4 dpf (A,B,E,F) and 5 dpf (C,D,G,H). (A,C,E,G) Arrows indicate *glucagon* expression in photomicrographs of whole larvae. (B,D,F,H) Confocal projections of islets. (I) 2 dpf embryos and 5 dpf larvae injected with control MO or *gcga* MO.

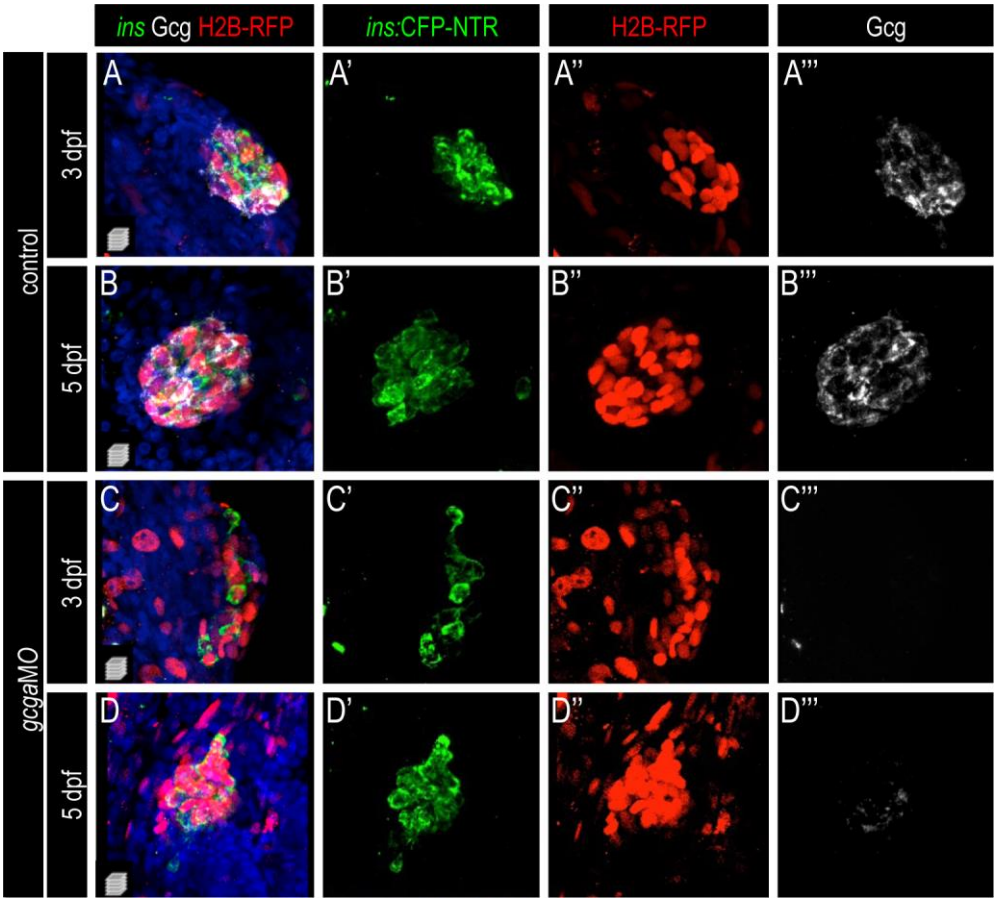

Figure S13. *gcga* knockdown decreases ventral pancreatic bud-derived β cell differentiation. (A-D’’’) Merged and single channel confocal projections of *Tg(ins:CFP-NTR)* islets injected with *H2B-RFP* mRNA alone (A-B’’’) or *H2B-RFP* mRNA + *gcga* MO that were stained for glucagon (white) ,CFP (green) and DNA (blue) at 3 dpf (A,C) and 5 dpf (B,D).

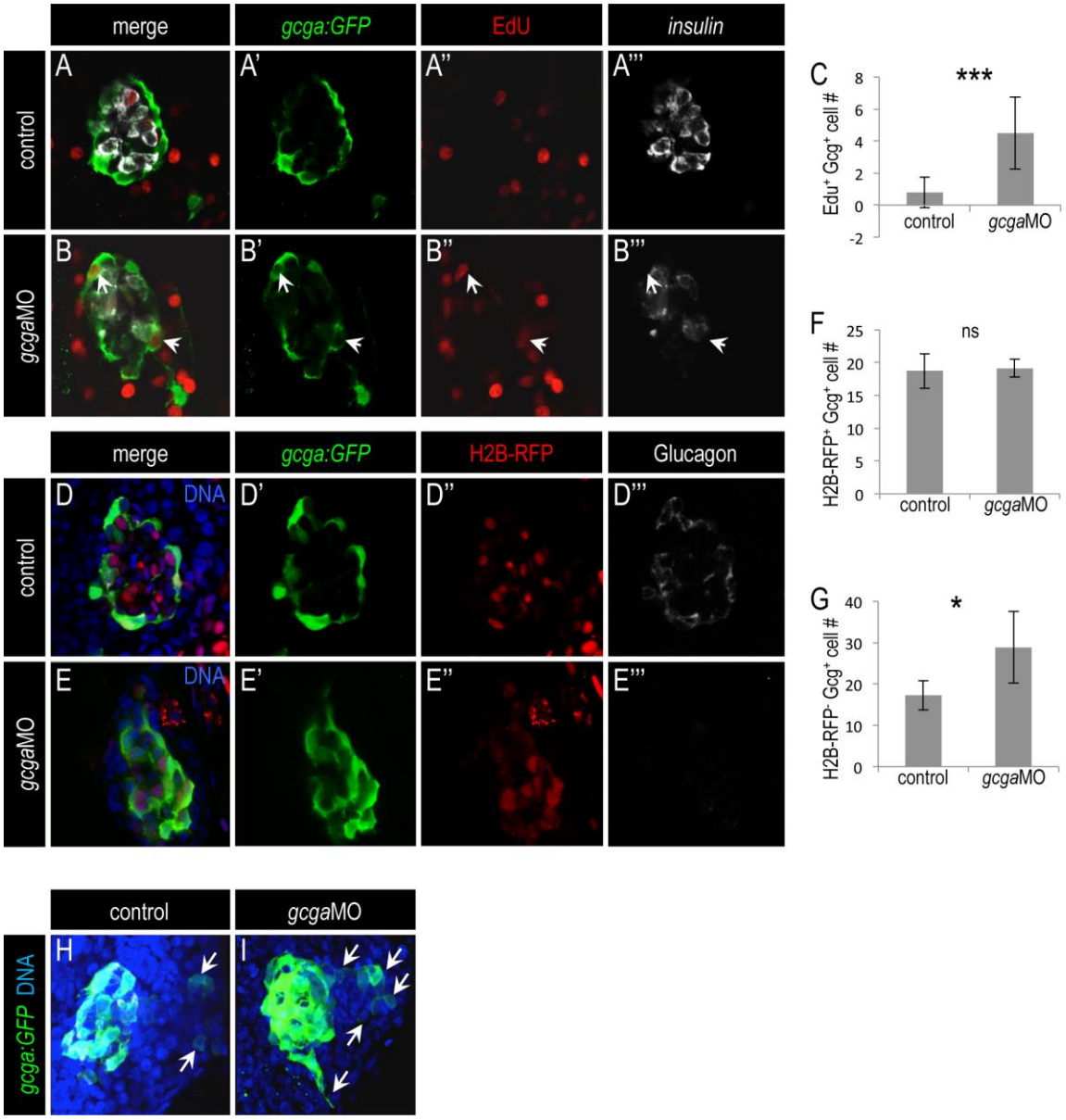

Figure S14. *gcga* knockdown increases α cell proliferation and neogenesis. (A-B) Merged and single channel confocal planes of 4 dpf control (A) and *gcga*MO-injected (B) *Tg(gcga:GFP)* islets labeled by insulin antibody (white) and EdU incorporation (red). (C) Quantification of EdU^{+} *gcga:GFP*$^{+}$ proliferating α cells in control (*n*=10) and *gcga*MO injected (*n*=12) islets. (D,E) Merged and single channel confocal planes of 3 dpf control (D) and *gcga*MO-injected (E) *Tg(gcga:GFP)* islets that were injected with H2B-RFP mRNA and labeled by Glucagon antibody (white). (F,G) Quantification of H2B-RFP^{+} *gcga:GFP*$^{+}$ dorsal bud-derived α cells (F) and H2B-RFP^{-} *gcga:GFP*$^{+}$ ventral bud-derived α cells (G) in control (*n*=7) and *gcga*MO (*n*=7) islets. (H-I) Confocal projections of 3 dpf control (H; *n*=7) and *gcga*MO-injected (I; *n*=7) *Tg(gcga:GFP)* islets. Arrows indicate newly forming *gcga:GFP*+ cells derived from pancreatic ducts.

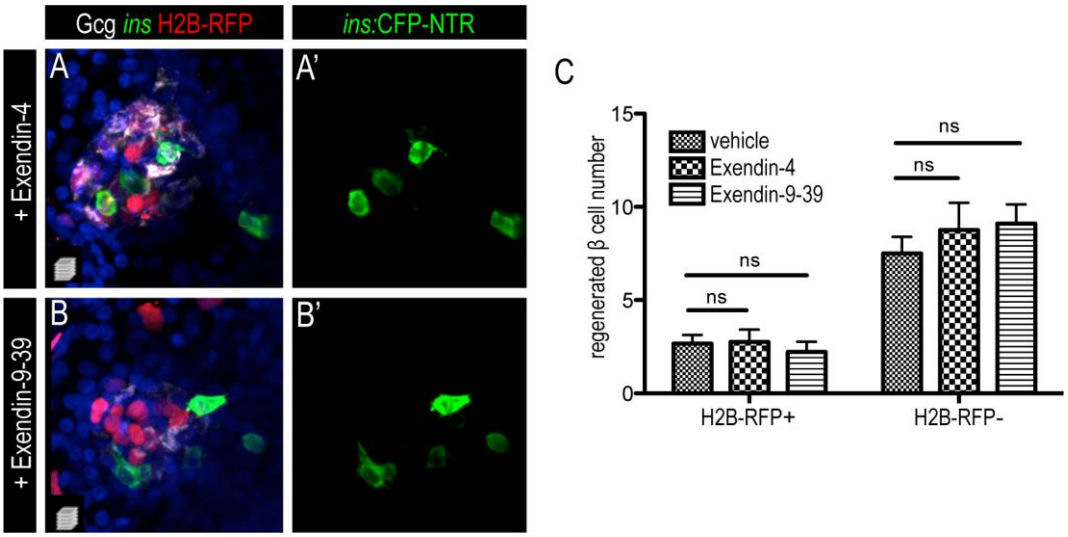

Figure S15. Glp-1 receptor agonist or antagonist treatment does not affect β cell regeneration. (A-B') Merged and single channel confocal projections of 5 dpf regenerating 1 dpa *H2B-RFP* mRNA injected islets that were treated with Exendin-4 (A) or Exendin-9-39 (B) during regeneration (comparable untreated control islets are shown in Fig. 4). (C) Quantification of H2B-RFP^{+} and H2B-RFP^{-} regenerated βcells in vehicle, Exendin-4, and Exendin-9-39 treated islets. Two-way ANOVA was used in C for statistical analysis.

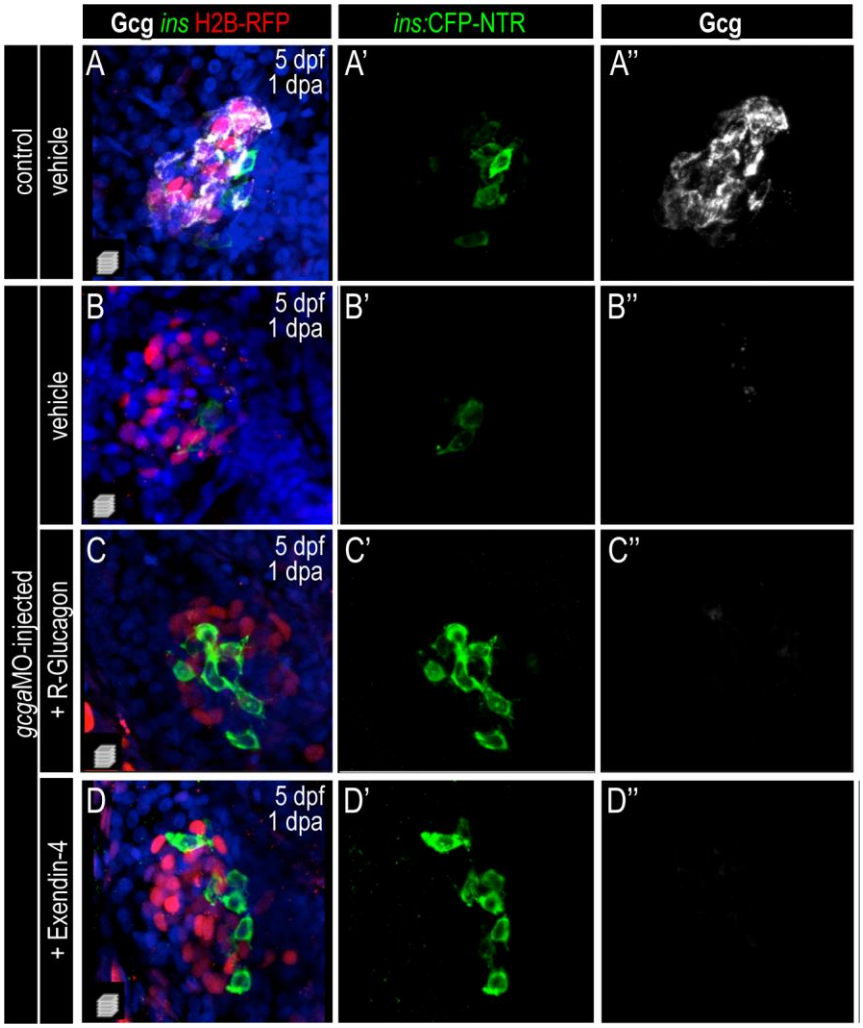

Figure S16. Glucagon or Exendin-4 injections rescue β cell regeneration in *gcga MO*-injected islets. (A-D'') Merged and single channel confocal projections of 5 dpf/1 dpa regenerating *H2B-RFP mRNA*-injected (red) islets that were not morpholino-injected (A), or injected with *gcgaMO* (B-D) and stained for CFP (*ins:CFP-NTR*; green), glucagon (white), and DNA (blue).

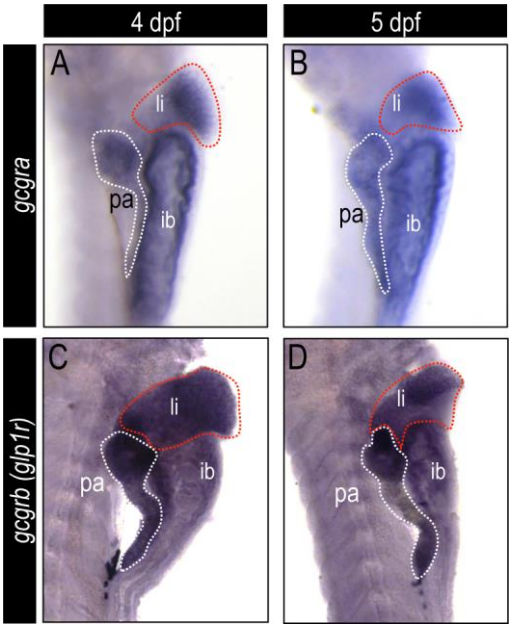

Figure S17. *glucagon receptor* and *glp-1 receptor* mRNAs are expressed in the larval pancreas. (A-D) Whole mount *in situ hybridization* showing regionally restricted expression of glucagon receptor (*gcgra*; A,B) and glp-1 receptor (*gcgrb/glp1r*; C,D) in the endodermal organs of 4 dpf (A,C) and 5 dpf (B,D) larvae. Note that both receptors are expressed throughout the pancreas, including exocrine and islet regions. Abbreviations: pa: pancreas; li: liver; ib: intestinal bulb.

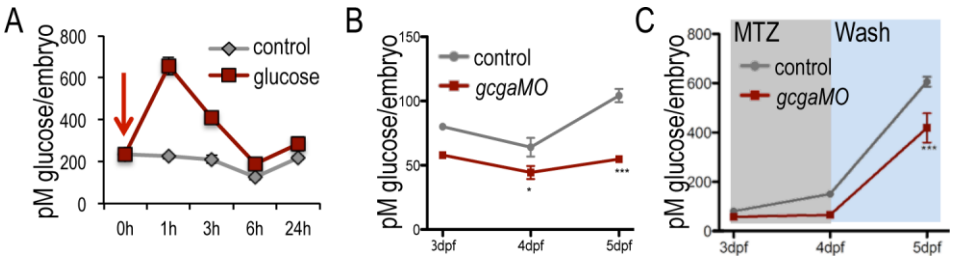

Figure S18. *glucagon* gene products regulate free glucose levels in zebrafish. (A) Free glucose levels measured periodically after mannose control (gray line) or glucose (red line) injection (arrow). (B) Free glucose measurement of control (gray line) and *gcga MO*-injected (red line) larvae at 3, 4 and 5 dpf. (C) Free glucose measurement in control uninjected and *gcgaMO*-injected *Tg(ins:CFP-NTR)* larvae in which βcells were ablated from 3 to 4 dpf. In both B and C, morpholino-injected zebrafish have diminished glucose levels. Two-way ANOVA was used in B and C for statistical analysis.

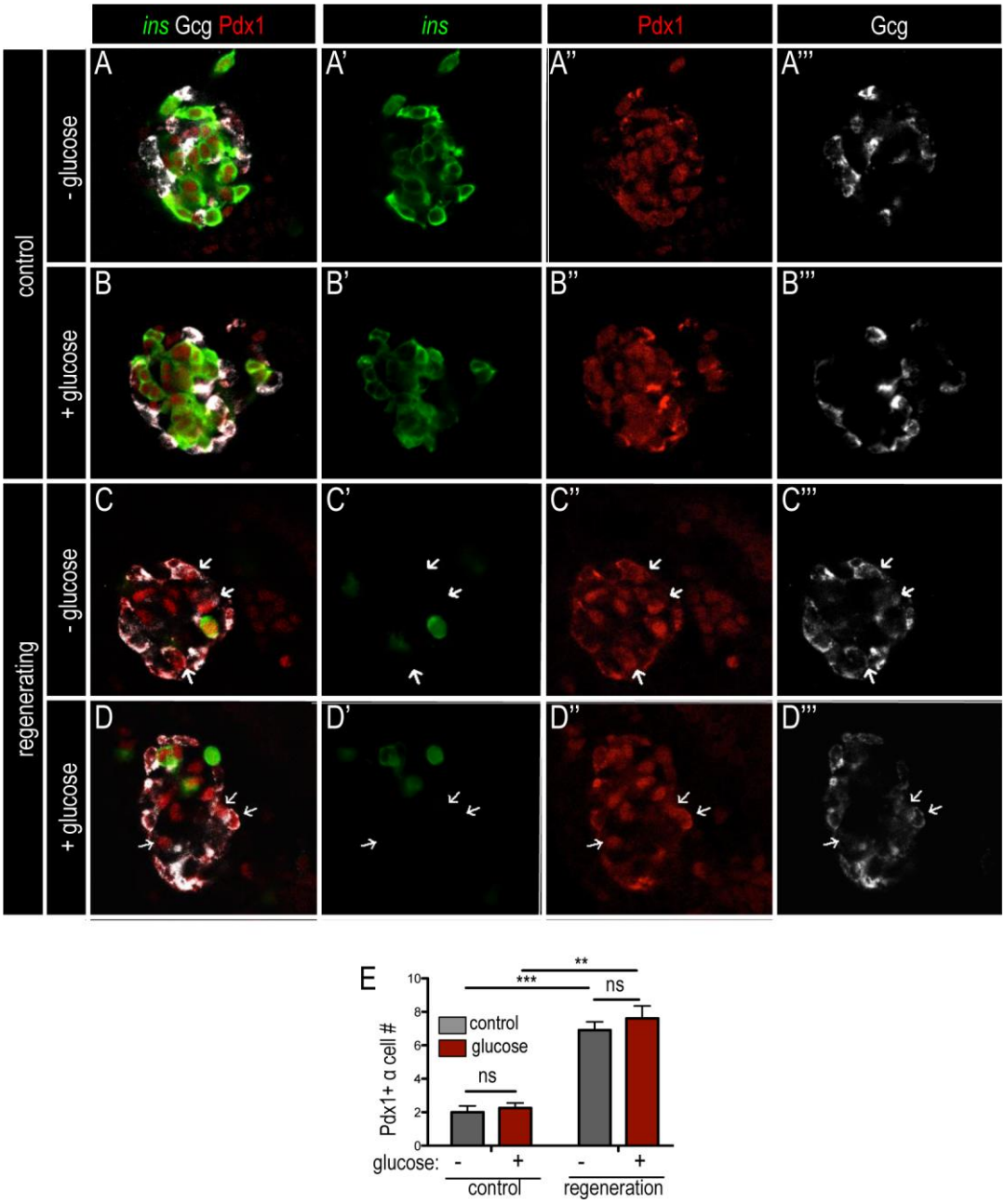

Figure S19. Quantity of Pdx1^{+} α cells is not affected by glucose injection. (A-D’’’) Merged and single channel confocal projections of 5 dpf non-ablated control (A-B’’’) and 1 dpa regenerating (C-D’’’) *Tg(ins:CFP-NTR)* islets that were not injected (A,C) or were injected with glucose (B,D) at 4 dpf. Islets were stained for Pdx1 (red), CFP (*ins:CFP-NTR*; green), and glucagon (white). Pdx1^{+} glucagon^{+} double positive cells are marked with white arrows in C,D. (E) Quantification of Pdx1 expression in αcells of intact and regenerating larvae was not altered by glucose injection; control group (*n=8*) and glucose treated group (*n=12*). Two-way ANOVA was used in E for statistical analysis.

Supplementary Table 1. Pancreatic gene expression in regenerating endoderm.

age		**gene**						
		insa	***gcga***	***arx***	***mafa***	***mafb***	***neurod1***	***ela3l***
0 dpa	**4 dpf**	-22.08**	+1.577**	-1.262	-1.335*	-1.801**	-1.189	-1.010
1 dpa	**5 dpf**	-39.43***	+2.00***	-1.317	+1.682***	-1.275	-1.324	+1.054
3 dpa	**7 dpf**	-10.45***	-1.15	-1.243	+1.686***	+1.022	+1.262*	-1.241*
Positive and negative value indicates fold increase or decrease of gene expression in regenerating endoderm compared with age matched un-ablated control. MTZ was added from 3 dpf to 4 dpf for ablation of βcells. *n*=3 for each group. Two way ANOVA analysis * p≤0.05, ** p≤0.01, *** p≤0.001								

Supplementary Table 2. Primers used for qPCR analyses.

gene	**strand**	**sequence**
lmnb1	sense	5’-ACCCGCGGCAAGAGAAAGCG
	antisense	5’-TCCTGCCATCGGCTGGTCCT
insa	sense	5’-TCTGCTTCGAGAACAGTGTG
	antisense	5’-GGAGAGCATTAAGGCCTGTG
gcga	sense	5’-AAGGCGACAGCACAAGCACA
	antisense	5’-GCCCTCTGCATGACGTTTGACA
arx	sense	5’-AAAAGCAAGTCGCCCACCGT
	antisense	5’-AATTTGGGCGGCAGGTGCATGT
mafa	sense	5’-ATTGTTCGCCGGGCTGTGTT
	antisense	5’-TGCTTTTGGCACAACCGGCA
mafb	sense	5’-CGCCAAACTGTGTTTGCGCTGA
	antisense	5’-AGGCGGCTTTAACGGGAGAAGT
neurod1	sense	5’-ACGCAGCGCTGTGATATACCGA
	antisense	5’-TCGCGTTCAACTGGGCGTTCAT
ela3l	sense	5’-GCTGAGCCTGTGACACTGAG
	antisense	5’-TCTCTGTGTGTTGGTTTTCTGG
trypsin	sense	5'-AGACCGTCTCTCTGCCTTCA
	antisense	5’- CAACACGCCATGATAACGAC
isl1	sense	5’-AGCAGCAGCAACCCAACGACAA
	antisense	5’-TGCACCTCCACTTGGTTTGCCT
opn1sw1	sense	5’-CCCAAATGGGCGTTCTACCT
	antisense	5’-CAAGGACCATCCCGTCACAA

Supplementary Table 3. Primers used for In Situ Hybridization.

glucagon	sense	5’-ATAAGCGAGGAGACGATCCA
	antisense	5’-GctaatacgactcactataggGCAATGAAGCCATCAGTTCTC
gcgr	sense	5’-GAGTGTCACCGCAGTTCAGT
	antisense	5’-GctaatacgactcactataggCTGTCCGTCTGCATCACACT
glp1r	sense	5’-CCGCTCATATTTGTGCTGCC
	antisense	5’-GctaatacgactcactataggAGCGGAGCCTTCATTGTTGA

Supplementary Table 4. Morpholino sequences

name	gene	morpholino sequence	dose
standard control MO	no target in *Danio rerio*	5'- CCTCT TACCT CAGTT ACAAT TTATA	4 or 8 ng
***arx*MO**	*arx* (NM_131384.1)	5'-TATCG TCGTC GTACT GACTG CTCAT	4 ng
***gcga*MO**	*gcga* (NM_001008595.3)	5'- GGCAA AATAC TGGAC GCCTT TCATT	8 ng

SUPPLEMENTARY MATERIALS AND METHODS

Zebrafish maintenance and strains: The following transgenic lines were used in the experiments: *TgBAC(neurod1:EGFP)* (Obholzer et al., 2008), *Tg(sox17:GFP)*^{s870} (Sakaguchi et al., 2006),*Tg(insa:Cre; cryaa:YFP)*^{s924} (Hesselson et al., 2009) ,*Tg(Ins:CFP-NTR)*^{s892} (Curado et al., 2007), *Tg(gcga:GFP)*^{ia1} (Pauls et al., 2007), *Tg(ins:dsRed)*^{m1018} (Anderson et al., 2009), *Tg(ins:Flag-NTR;cryaa:mCherry)*^{s950} (Andersson et al., 2012), and *Tg(hs:loxp-mCherry-STOP-loxp-H2BGFP)*^{s925} (Hesselson et al., 2009). *Tg(gcga:Cre; cryaa:YFP)*^{s962} and *Tg(sst2:Cre; cryaa:YFP)*^{s963} were constructed and generated by meganuclease transgenesis as described (Hesselson et al., 2009). To construct the *Cre* transgenes, *glucagon* promoter (gift of F. Argenton) or *sst2* promoter was subcloned into *ins:Cre; cryaa:Venus*. A 2 kb *sst2* promoter region was amplified from the CH211-232H16 zebrafish genomic clone (CHORI) using the oligos: 5'-GCATG AATTC AGCCT CTATG TCCTT CGTCT and 5'-GCATG GATCC TGCTG CTTCT TTAAC TCAG.

Detection of protein, mRNA, and cell proliferation: The following antibodies were used: chicken anti-GFP (1:500; Aves Labs #GFP-1020); guinea pig anti-insulin (1:100; Life Technologies #180067); mouse anti-glucagon (1:100; Sigma #G2654); rabbit anti-somatostatin (1:100 Serotec # 8330-0154); rabbit anti-dsRed (1:250; Clontech # 632496); mouse anti-PCNA (1:100; Abcam #PC10); rabbit anti-PHH3 (1:250; Cell Signaling #9701), guinea anti-Pdx1 (1:50 gift of Dr. C. Wright). Alexa Fluor-conjugated antibodies were used for visualization (1:500; Life Technologies). *glucagon* probe template was PCR amplified from cDNA with 5'-ATAAG CGAGG AGACG ATCCA and 5'-GCTAA TACGA CTCAC TATAG GGCAA TGAAG CCATC AGTT CTC primers. For quantitative PCR, we enriched endodermal organs by manual dissection of the digestive system with watchmakers forceps, which included pancreas, intestine, and liver from 4, 5, and 7 dpf larvae. 20-30 endoderm

preparations were pooled for each condition to minimize variability between dissections. mRNA was extracted with Trizol (Life Technologies) and reverse transcribed with iScript (BioRad). The Mastercycler Realplex PCR system (Eppendorf) was used with Sybr Green mix and Mytaq (BioLine) to generate Ct values. The relative expression of each sample was determined by normalizing to *lmnb1* using the relative standard curve method (Hesselson et al., 2009).

Microinjections: *H2B-RFP* mRNA was transcribed with SP6 mMessage machine kit (Invitrogen), and 100 pg were injected into zygotes. Anti-dsRed (Clontech) and Alexa568 antibodies (Life Technologies) were used to amplify the signal. The following antisense morpholinos (Gene Tools LLC) were injected into zygotes: control MO (4 or 8 ng), *gcga*MO (8 ng), and *arxa*MO (4 ng). Specificity of morpholino knockdown was addressed in multiple ways: First, significant off-target effects were unlikely in either *glucagon* or *arxa* morphants, as we observed no gross morphological defects, which are characteristic of such off-target and other non-specific toxic effects in morphants, (Figures S10C, S12I). Secondly, *gcga* and *arxa* morpholino phenotypes recapitulated phenotypes seen in mouse with knockdown of components of the glucagon signaling pathway (Hayashi et al., 2009; Vuguin and Charron, 2011) or Arx (Collombat et al., 2003). Thirdly, regeneration of beta cells in the *gcga* knockdown was rescued by injection of recombinant human Glucagon peptide or the Glp1 receptor agonist Exendin-4, but not the Glp1 receptor antagonist Exendin9-39 (Fig. 5A-G; S16). Finally, injection of a second *arxa* morpholino (*arxa*MO2 = 5'- ATGTT TGTAT CGTCC TCAGT CGTGC) produced identical phenotype in the islet (R.M.A., unpublished). To address morpholino efficacy, *gcga*MO eliminated glucagon protein in the islet (Fig. 4D'), and *arxa*MO specifically eliminated expression of an *arxa-GFP* DNA reporter construct that was co-injected into zygotes (R.M.A. unpublished).

Drug/chemical treatments: For βcell ablation, *Tg(ins:CFP-NTR)*^{s892} *or Tg(ins:Flag-NTR)*^{s950} animals were incubated in 0.1% DMSO (Sigma) ± 10 mM Metronidazole (MTZ, Sigma) in egg water. After ablation (generally 24 hrs), embryos were washed extensively with egg water, and recovered for 1-16 days. For peptide treatments, a mixture of KCl (0.2M), phenol red (0.1%), and either vehicle, recombinant human Glucagon (Sigma), Exendin-4 (Sigma), Exendin9-39 (Sigma), glucose, or mannose was injected into the pericardial sac of each embryo following ablation. The total mass of each drug injected was 20 pg. Glucose or mannose was injected with a final mass of 10 ng/larva. After injection, embryos recovered at 28˚C for 5 h before ablation.

SUPPLEMENTARY REFERENCES:

Anderson, R. M., Bosch, J. A., Goll, M. G., Hesselson, D., Dong, P. D. S., Shin, D., Chi, N. C., Shin, C. H., Schlegel, A., Halpern, M. et al. (2009). Loss of Dnmt1 catalytic activity reveals multiple roles for DNA methylation during pancreas development and regeneration. In *Dev. Biol.*, vol. 334, pp. 213-223.

Andersson, O., Adams, B. A., Yoo, D., Ellis, G. C., Gut, P., Anderson, R. M., German, M. S. and Stainier, D. Y. R. (2012). Adenosine signaling promotes regeneration of pancreatic β cells in vivo. In *Cell metabolism*, vol. 15, pp. 885-894.

Collombat, P., Mansouri, A., Hecksher-Sorensen, J., Serup, P., Krull, J., Gradwohl, G. and Gruss, P. (2003). Opposing actions of Arx and Pax4 in endocrine pancreas development. *Genes Dev* **17**, 2591-2603.

Curado, S., Anderson, R. M., Jungblut, B., Mumm, J., Schroeter, E. and Stainier, D. Y. R. (2007). Conditional targeted cell ablation in zebrafish: a new tool for regeneration studies. In *Dev. Dyn.*, vol. 236, pp. 1025-1035.

Hayashi, Y., Yamamoto, M., Mizoguchi, H., Watanabe, C., Ito, R., Yamamoto, S., Sun, X. y. and Murata, Y. (2009). Mice Deficient for Glucagon Gene-Derived Peptides Display Normoglycemia and Hyperplasia of Islet -Cells But Not of Intestinal L-Cells. In *Mol. Endocrinol.*, vol. 23, pp. 1990-1999.

Hesselson, D., Anderson, R. M., Beinat, M. and Stainier, D. Y. R. (2009). Distinct populations of quiescent and proliferative pancreatic beta-cells identified by HOTcre mediated labeling. In *Proceedings of the National Academy of Sciences*, vol. 106, pp. 14896-14901.

Obholzer, N., Wolfson, S., Trapani, J. G., Mo, W., Nechiporuk, A., Busch-Nentwich, E., Seiler, C., Sidi, S., Söllner, C., Duncan, R. N. et al. (2008). Vesicular glutamate transporter 3 is required for synaptic transmission in zebrafish hair cells. In *Journal of Neuroscience*, vol. 28, pp. 2110-2118.

Pauls, S., Zecchin, E., Tiso, N., Bortolussi, M. and Argenton, F. (2007). Function and regulation of zebrafish nkx2.2a during development of pancreatic islet and ducts. In *Dev. Biol.*, vol. 304, pp. 875-890.

Sakaguchi, T., Kikuchi, Y., Kuroiwa, A., Takeda, H. and Stainier, D. Y. (2006). The yolk syncytial layer regulates myocardial migration by influencing extracellular matrix assembly in zebrafish. *Development* **133**, 4063-4072.

Vuguin, P. M. and Charron, M. J. (2011). Novel insight into glucagon receptor action: lessons from knockout and transgenic mouse models. *Diabetes, obesity & metabolism* **13 Suppl 1**, 144-150.